Journal of Crystal Growth 315 (2011) 216–219

Contents lists available at ScienceDirect

Journal of Crystal Growth

journal homepage: www.elsevier.com/locate/jcrysgro

High quality AlGaN epilayers grown on sapphire using SiN$_x$ interlayers

K. Forghani [a],*, M. Klein [a], F. Lipski [a], S. Schwaiger [a], J. Hertkorn [a], R.A.R. Leute [a], F. Scholz [a], M. Feneberg [b], B. Neuschl [b], K. Thonke [b], O. Klein [c], U. Kaiser [c], R. Gutt [d], T. Passow [d]

[a] Institut für Optoelektronik, Universität Ulm, Albert-Einstein-Allee 45, 89069 Ulm, Germany
[b] Institut für Quantenmaterie/Gruppe Halbleiterphysik, Universität Ulm, 89069 Ulm, Germany
[c] Materialwissenschaftliche Elektronenmikroskopie, Universität Ulm, 89081 Ulm, Germany
[d] Fraunhofer-Institut für Angewandte Festkörperphysik, Tullastraße 72, 79108 Freiburg, Germany

A R T I C L E I N F O

Available online 8 September 2010

Keywords:
A1. Atomic force microscopy
A1. High resolution X-ray diffraction
A1. Photoluminescence
A3. *In situ* nano-masking
A3. Metalorganic vapor phase epitaxy
B1. Aluminium gallium nitride

A B S T R A C T

We have investigated the optimization of Al$_{0.2}$Ga$_{0.8}$N layers directly grown on sapphire by metalorganic vapor phase epitaxy (MOVPE). The quality of the AlGaN epilayers was improved by *in situ* nano-masking employing ultra-thin SiN$_x$ interlayers. Transmission electron microscopy (TEM) investigations reveal an enormous reduction of edge-type dislocations by SiN$_x$ nano-masking. Furthermore, formation of bundles of dislocations converging to the surface is visible, leading to large areas up to 1 μm in size on the surface which are almost defect free. The SiN$_x$ surface coverage was carefully optimized resulting in narrower (1 0 2)-reflections of high resolution X-ray diffraction (HRXRD), down to full width at half maximum (FWHM) values of 570 arcsec, in addition to narrow symmetric HRXRD reflections down to FWHM of 150 arcsec. Structures with double SiN$_x$ interlayer revealed even higher quality of the epilayers with a FWHM of 440 arcsec for the (1 0 2)-reflection. A series of GaN–AlGaN multi-quantum wells were grown on such high quality templates. The MQWs show a significant decrease in peak widths and also an increase in the luminescence intensity. Furthermore, these templates have been used as buffer layers for ultraviolet light-emitting diodes emitting at 350 nm.

1. Introduction

The metalorganic vapor phase epitaxy (MOVPE) of AlGaN has attracted strong research interest due to the applicability of AlGaN for ultraviolet light-emitting diodes (UV-LEDs) and laser diodes. AlGaN layers grown directly on sapphire typically exhibit a large number of threading dislocations (TDs), which mainly occur in the form of edge-type TDs [1]. These TDs are the main limiting factor for the performance of UV light-emitting devices [2,3].

A common method to reduce the TD density in (Al,Ga)N layers is the use of epitaxial lateral overgrowth (ELO). Different ELO techniques with *ex situ* substrate patterning are widely used to grow high quality GaN layers [4–6] and have also been adapted to AlGaN layers [7,8]. However, long *ex situ* masking procedures and the presence of localized TDs in the window regions are typical drawbacks of ELO. Moreover, a relatively thick overgrowth of the mask is essential to coalesce the wing areas.

In situ ELO techniques, especially in small scales, are of general interest due to the possibility to overcome the drawbacks of ELO while keeping its advantages. It has been shown by Tanaka et al. [9] that SiN$_x$ intermediate layers deposited *in situ* are an effective tool to grow high quality GaN epilayers. However, Engl et al. [10] observed that SiN$_x$ interlayers do not reveal any visible improvement in crystal quality of AlGaN layers, since AlGaN does not grow as selective as GaN [11].

Recently, we succeeded in the implementation of SiN$_x$ for AlGaN layers with 20% Al content and developed an appropriate model for the effect of SiN$_x$ interlayers on the reduction of edge-type TD in AlGaN [12]. Here, we report on a systematical optimization of the position and thickness of the SiN$_x$ interlayers using the full widths at half maximum (FWHM) of high-resolution X-ray diffraction rocking curves (HRXRD-RCs) as figures of merit.

2. Experimental procedure

All samples investigated in this study were grown on 2 in (0 0 0 1) sapphire substrates with a miscut of 0.3° towards the *a*-plane, in a low-pressure horizontal reactor (Aixtron AIX-200/4 RF-S). Trimethylgallium (TMGa) and trimethylaluminum (TMAl) were used as group-III precursors, and ammonia as group-V precursor. The Al content in our samples was typically about 20% as confirmed by photoluminescence (PL). The process temperature was set to 1120 °C. As for our high quality GaN layers [13], we used a nucleation layer (NL) of oxygen doped AlN with a thickness

---

* Corresponding author. Tel.: +49 7315026039; fax: +49 7315026049.
E-mail address: kamran.forghani@uni-ulm.de (K. Forghani).

0022-0248/$ - see front matter © 2010 Elsevier B.V. All rights reserved.
doi:10.1016/j.jcrysgro.2010.08.044

of about 25 nm. Silane was used for the *in situ* deposition of the SiN_x interlayers [14]. The surface coverage of the SiN_x interlayers is controlled by the variation of the deposition time.

HRXRD-RCs for crystal quality evaluation were performed on a Siemens D5000 equipped with a four bounce Ge (2 2 0) monochromator at the primary beam side in addition to a scintillation detector. In order to monitor the dislocation propagation, transmission electron micrsocope (TEM) investigations were carried out in weak beam dark field (WBDF) mode on a Philips CM-20 microscope after standard sample preparation including mechanical polishing and low-angle argon thinning [12]. Surface morphologies were evaluated by atomic force microscopy (AFM) operated in tapping mode.

A series of AlGaN/GaN (8 × 7 nm/3 nm) MQW were grown without growth interruption on buffer layers with different SiN_x modifications. The cathodoluminescence (CL) signal was detected at a sample temperature of 10 K. On the best achieved template, AlGaN/GaN single quantum well (SQW) UV-LEDs with an emission wavelength of 350 nm were grown after transfer into a similar MOVPE reactor. Electroluminescence (EL) measurements were taken on-wafer using evaporated Ni/Al/Ni/Au p-contacts and In bumps as n-contacts [3].

3. Results

As a reference for the following investigations, an AlGaN epilayer with 20% Al content was grown with a thickness of 2.5 μm. The HRXRD-RCs showed a very narrow symmetric (0 0 2)-reflection FWHM of 57 arcsec. This indicates a low density of screw-type dislocation, since the symmetric HRXRD-RCs are mainly broadened by screw/mixed-type dislocations, although other factors may also be responsible for such very narrow peaks [15].

On the other hand, the very broad asymmetric (1 0 2)-reflection FWHM of 1590 arcsec reflects the high density of edge-type dislocations [16]. Therefore, our main interest in this work was to grow AlGaN epilayers with as narrow as possible asymmetric HRXRD reflections corresponding to a low density of edge-type TDs.

3.1. SiN_x nano-mask directly on the NL

In order to find out the optimal coverage of the SiN_x nano-mask, we first deposited the mask directly on the NL and grew nominally 1 μm AlGaN above the mask. The deposition time of the SiN_x interlayer was varied between 2 and 5 min to achieve sub-monolayer surface coverage, which is necessary to obtain a nano-mask for optimal growth results [9]. The sample with deposition time of 4 min had the narrowest asymmetric HRXRC-RC with a FWHM of 685 arcsec revealing an enormous reduction of the edge-type TD density due to the SiN_x nano-masking compared to the AlGaN epilayers without SiN_x interlayers (see Table 1).

The AFM evaluations have shown that the samples with deposited SiN interlayer have rougher surfaces compared to the reference sample with RMS-value of 1 nm in 10 μm × 10 μm scans (see Table 1). It has to be mentioned that the symmetric peak widths are broadened compared to the reference sample without SiN_x interlayers. This is explained by the distortion of the atomic planes in (0 0 1) direction by the SiN_x interlayers in addition to the reduced layer thickness. Hence, the broadening of (0 0 2) HRXRD-RCs does not necessarily mean that a high number of screw-type TDs has been introduced due to the existence of the SiN_x interlayer.

Table 1
Effect of SiN_x interlayer deposition time on (1 0 2) and (0 0 2) HRXRC-RCs and AFM surface roughness evaluations (deposition directly on the NL).

SiN_x (min)	(1 0 2) FWHM (arcsec)	(0 0 2) FWHM (arcsec)	RMS (nm)
2	1991	210	1.8
3	1240	378	1.9
4	685	260	6.3
5	961	435	6

3.2. SiN_x nano-mask 150 nm above the NL

Another parameter which can be investigated for SiN_x nano-masks, is the position of the SiN_x deposition. We chose structures similar to Section 3.1 and just inserted 150 nm AlGaN between the NL and the SiN_x nano-mask. We did not intentionally change the growth conditions of the AlGaN below the SiN_x nano-mask in comparison to the overgrown AlGaN. A similar optimization of the mask coverage by varying the deposition time of the SiN_x between 3 and 8 min was carried out. The best results within the series could be obtained for a deposition time of 6 min with a (1 0 2)-FWHM of 571 arcsec (see Table 2).

Obviously, the improvement was more significant as we observed in Section 3.1, when the SiN_x was deposited directly on the NL. A possible explanation could be that the SiN_x deposition is affected differently by the AlGaN surface compared to the AlN:O surface of the NL in the previous experiment. However, we also grew more complicated structures, e.g. deposition of two SiN_x interlayers with the first one directly on the NL and the second one after 300 nm AlGaN (total thickness of 1.4 μm). This double-SiN_x interlayer structure is the best we could achieve with a FWHM of the (1 0 2)-reflection of 440 arcsec.

For a better understanding of the dislocation propagation behavior in such structures with SiN_x nano-mask, we performed TEM investigations. According to Fig. 1, edge-type TDs (the main existing TDs) are generally stopped by the SiN_x interlayer. TDs in some regions are merged or bent, creating bundles of dislocations reaching the surface. Thus, this bundling increases the dislocation free surface areas effectively. In addition, dislocations are forced to annihilate by the SiN_x layer. Fairly large defect-free areas with diameters in the range of few micrometers in lateral size could be observed.

3.3. Overgrowth thickness

When the SiN_x coverage is higher, the surface becomes rougher (especially due to the formation of hexagonally shaped nano-islands with tilted m-plane facets). This is evident from AFM roughness evaluations in 10 μm × 10 μm scans (see Table 2). Whenever the mask coverage is higher, consequently, more overgrowth thickness is necessary in order to coalesce the initiated facets. Therefore, we carried out a series of investigations concerning the effect of the overgrown layer thickness after the

Table 2
Effect of SiN_x deposition time on (1 0 2) and (0 0 2) HRXRC-RCs and AFM surface roughness evaluations (deposition 150 nm after the NL).

SiN_x (min)	(1 0 2) FWHM (arcsec)	(0 0 2) FWHM (arcsec)	RMS (nm)
3:30	1789	115	2
4	1212	160	6
4:30	999	183	8
5	645	321	15
6	571	343	25
7	645	308	23
8	818	301	58

SiN_x mask on the surface topography. A sample with SiN_x deposition time of 6 min after 150 nm AlGaN was chosen. Fig. 2 shows the surface topography and roughness evaluations done by AFM. After 2.5 μm overgrowth, we achieved sub-nm roughness values which was even less than for our reference sample which showed 1 nm roughness.

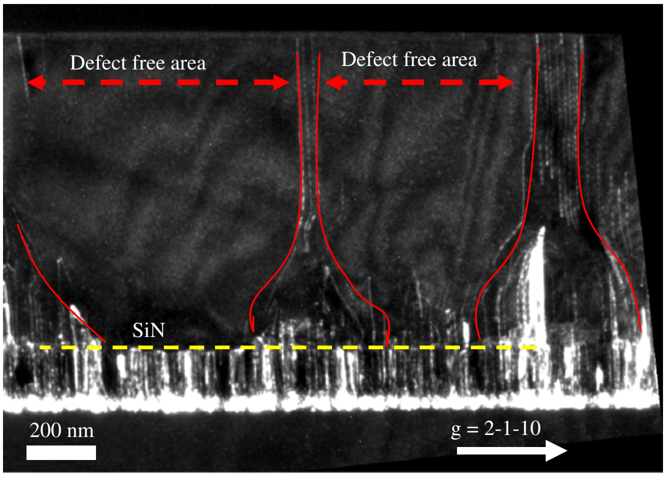

Fig. 1. WBDF-TEM from cross-section of a sample with 4 min SiN_x deposited 150 nm above NL with 1 μm overgrowth. Edge-type TDs can reach the surface mostly in the form of bundles of dislocations (solid red lines), but rarely separately. (For interpretation of the references to color in this figure legend, the reader is referred to the web version of this article.)

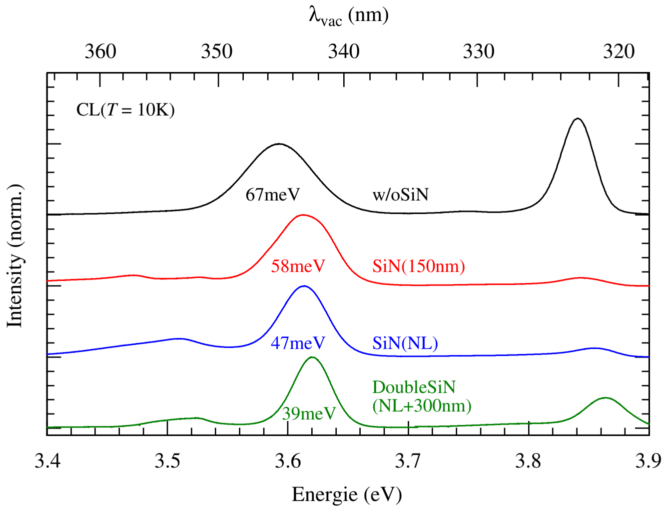

Fig. 3. Normalized CL for reference sample (without SiN_x interlayer) and some high quality AlGaN layers with SiN_x interlayer.

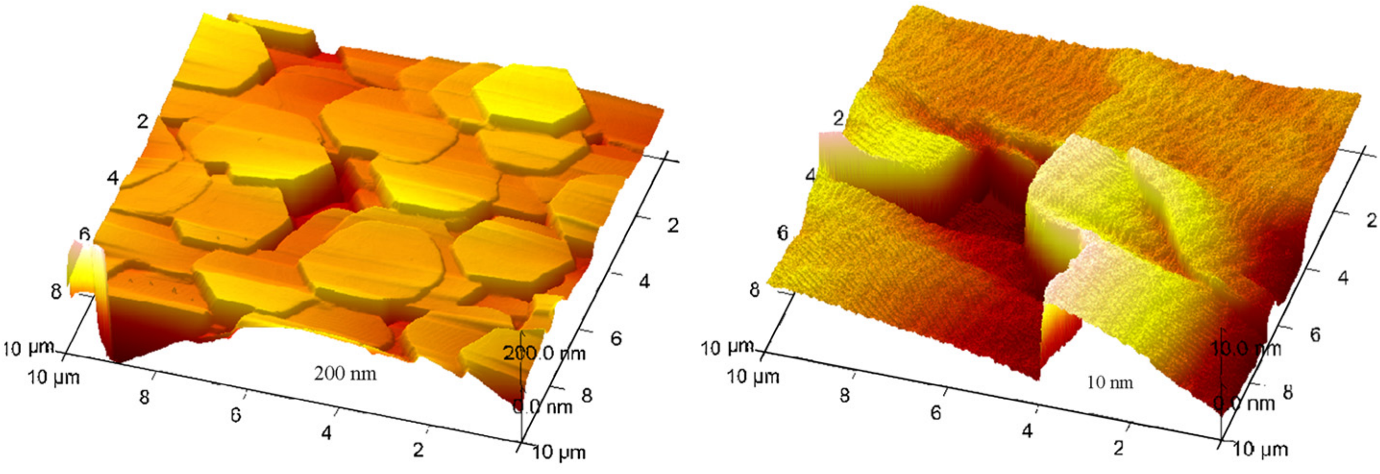

RMS = 25nm after 1μm overgrowth

RMS = 3nm after 1.8μm overgrowth

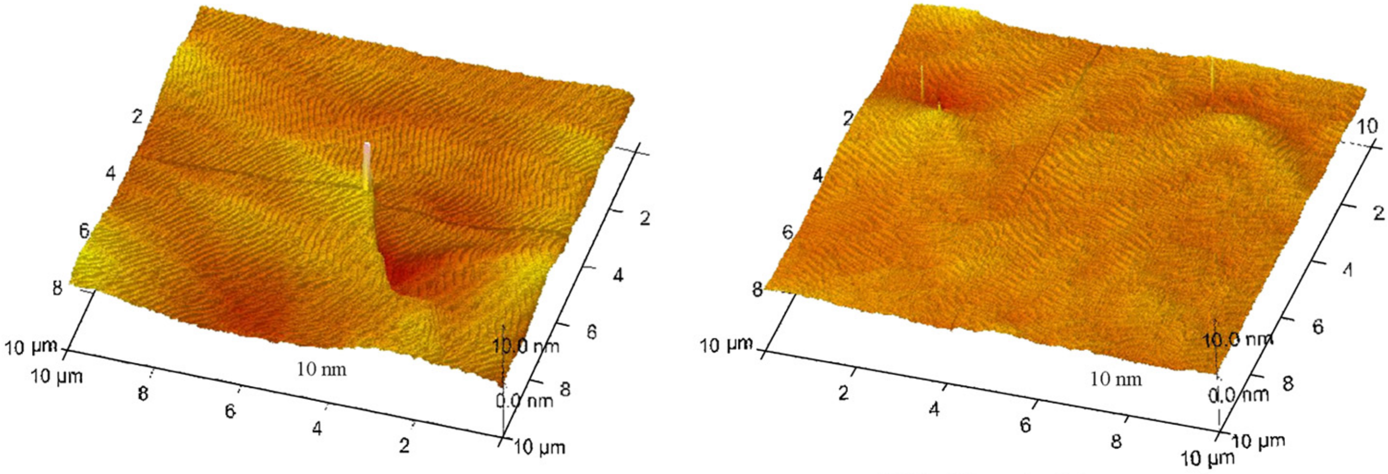

RMS = 0.8 nm after 2.5μm overgrowth

RMS = 0.3 nm after 3.4μm overgrowth

Fig. 2. Surface topography evaluations after different overgrowth of SiN_x mask (6 min deposited) with AlGaN (20%).

As already indicated in Section 3.1, the symmetric HRXRD-RCs are broadened by the relatively low thickness of the investigated samples described above. The overgrowth of the samples decreases the symmetric (0 0 2)-RC peak to a FWHM-value of around 150 arcsec. Moreover, the asymmetric (1 0 2)-RC peak FWHM is decreased down to a value of 443 in for the sample with 3.4 μm overgrowth.

3.4. QW luminescence and UV-LED performance

AlGaN/GaN MQW structures were grown on different buffer layers to evaluate the effect of the improved epilayer quality due to the SiN_x interlayers on the luminescence properties. On the reference sample (AlGaN epilayer without SiN_x interlayer), the MQW cathodoluminescence (CL) intensity at about 3.6 eV is weaker than that of the AlGaN barrier at about 3.85 eV. The FWHM of the MQW emission is 67 meV (see Fig. 3). However, MQWs grown on the layers with a SiN_x interlayer (4 min deposited 150 nm above the NL) showed much more intense CL from the MQWs compared to that of the barrier. The FWHM is reduced to 58 meV, although a slight peak splitting probably due to MQW thickness variations is observable. The MQW with the SiN_x interlayer directly on the NL (4 min deposited) showed single-peak emission with an even narrower FWHM of 47 meV. The double-SiN_x interlayer structure with the first one on the NL and the second one after 300 nm AlGaN exhibits the narrowest luminescence spectrum with a FWHM of 42 meV.

Finally, simple AlGaN/GaN SQW UV-LED structures emitting at 350 nm were grown on this double-SiN_x interlayer buffer layer. They demonstrated a typical output power of 1 mW at 40 mA measured on-wafer, which corresponds to a 20-fold increase compared to similar LEDs grown without defect reduction by SiN_x interlayers.

4. Conclusion

In situ deposited SiN_x nano-masking is demonstrated to be an effective technique to reduce the edge-type TD density in MOVPE grown AlGaN with an Al content of 20%. The dislocations are either completely stopped after the SiN_x nano-mask, or are converging towards the surface in the forms of bundles leading to larger dislocation free areas on the surface. The optimization of the position and thickness of the SiN_x interlayer results in significantly reduced asymmetric FWHM of the HRXRD-RCs. Sufficiently thick overgrowth of the samples leads to sub-nm surface roughness. Furthermore, MQWs grown on these buffer layers show improved luminescence properties. Double-SiN_x interlayer buffer layers have also been used as templates for UV-LEDs emitting at 350 nm, which demonstrated a typical output power of 1 mW at 40 mA measured on-wafer.

Acknowledgements

This work was financially supported by the German Federal Ministry of Education and Research (BMBF) within the framework of the ‘‘Deep UV-LED’’ project. AFM evaluations by R. Xue and M. Gharavipour are gratefully acknowledged.

References

[1] A. Khan, K. Balakrishnan, T. Katona, Nat. Photonics 2 (2008) 77.
[2] T. Okimoto, M. Tsukihara, K. Kataoka, A. Kato, K. Nishino, Y. Naoi, S. Sakai, Phys. Status Solidi C 5 (2008) 3066.
[3] R. Gutt, L. Kirste, T. Passow, M. Kunzer, K. Köhler, J. Wagner, Phys. Status Solidi B 247 (2010) 1710.
[4] K. Hiramatsu, K. Nishiyama, M. Onishi, H. Mizutani, M. Narukawa, A. Motogaito, H. Miyake, Y. Iyechika, T. Maeda, J. Cryst. Growth 221 (2000) 316.
[5] F. Habel, P. Brückner, F. Scholz, J. Cryst. Growth 272 (2004) 515.
[6] C.I.H. Ashby, C.C. Mitchell, J. Han, N.A. Missert, P.P. Provencio, D.M. Follstaedt, G.M. Peake, L. Griego, Appl. Phys. Lett. 77 (2000) 3233.
[7] R. Matsuoka, T. Okimoto, K. Nishino, Y. Naoi, S. Sakai, J. Cryst. Growth 311 (2009) 2847.
[8] K. Iida, T. Kawashima, M. Iwaya, S. Kamiyama, H. Amano, I. Akasaki, A. Bandoh, J. Cryst. Growth 298 (2007) 265.
[9] S. Tanaka, M. Takeuchi, Y. Aoyagi, Jpn. J. Appl. Phys. 39 (2000) 831.
[10] K. Engl, M. Beer, N. Gmeinwieser, U.T. Schwarz, J. Zweck, W. Wegscheider, S. Miller, A. Miler, H.J. Lugauer, G. Brüderl, A. Lell, V. Härle, J. Cryst. Growth 289 (2006) 6.
[11] Y. Kato, S. Kitamura, K. Hiramatsu, N. Sawaki, J. Cryst. Growth 144 (1994) 133.
[12] O. Klein, J. Biskupek, U. Kaiser, K. Forghani, S.B. Thapa, F. Scholz, J. Phys.: Conf. Ser. 209 (2010) 012018.
[13] J. Hertkorn, P. Brückner, S.B. Thapa, T. Wunderer, F. Scholz, M. Feneberg, K. Thonke, R. Sauer, M. Beer, J. Zweck, J. Cryst. Growth 308 (2007) 30.
[14] J. Hertkorn, F. Lipski, P. Brückner, T. Wunderer, S.B. Thapa, F. Scholz, A. Chuvilin, U. Kaiser, M. Beer, J. Zweck, J. Cryst. Growth 310 (2008) 4867.
[15] J. Bläsing, A. Krost, J. Hertkorn, F. Scholz, L. Kirste, A. Chuvilin, U. Kaiser, J. Appl. Phys. 105 (2009) 033504.
[16] S.B. Thapa, J. Hertkorn, F. Scholz, G.M. Prinz, R.A.R. Leute, M. Feneberg, K. Thonke, R. Sauer, O. Klein, J. Biskupek, U. Kaiser, J. Cryst. Growth 310 (2008) 4939.